学　位　論　文

Anti-diabetic drug metformin inhibits cell proliferation and tumor growth in gallbladder cancer via G0/G1 cell cycle arrest

香川大学大学院医学系研究科
分子情報制御医学専攻

山下　拓磨

Anti-diabetic drug metformin inhibits cell proliferation and tumor growth in gallbladder cancer via G0/G1 cell cycle arrest

Takuma Yamashita[a], Kiyohito Kato[a], Shintaro Fujihara[a], Hisakazu Iwama[b], Asahiro Morishita[a], Hiroki Yamana[a], Kiyoyuki Kobayashi[a], Hideki Kamada[a], Taiga Chiyo[a], Hideki Kobara[a], Kunihiko Tsutsui[d], Keiichi Okano[c], Yasuyuki Suzuki[c], and Tsutomu Masaki[a]

Affiliations:

[a]Department of Gastroenterology and Neurology, [b]Life Science Research Center, and [c]Gastroenterological Surgery (Faculty of Medicine), Kagawa University, Japan

1750-1 Ikenobe, Miki-cho, Kita-gun, Kagawa 761-0793, Japan

[d]Department of Health Sciences, Faculty of Medicine, Kagawa University, Japan

Corresponding author: Takuma Yamashita, MD

Department of Gastroenterology and Neurology,

Kagawa University Faculty of Medicine / Graduate School of Medicine

1750-1 Ikenobe, Miki-cho, Kita-gun, Kagawa 761-0793, Japan

Tel: +81-87-891-2156; Fax: +81-87-891-2158

E-mail: gcz32vg30@med.kagawa-u.ac.jp

Abbreviations: GBC, gallbladder cancer; miRNAs, microRNAs; CCK-8, cell counting kit; AMPK, AMP-activated protein kinase; RTK, receptor tyrosine kinase; Eph, Erythropoietin-producing human hepatocellular carcinoma cell; Tie 2, tyrosine kinase with Ig and EGF homology domain-2; ALK, anaplastic lymphoma kinase; PYK, proline-rich tyrosine kinase; TIMP-1, tissue inhibitor of metalloproteinases-1

Running title: YAMASHITA *et al*: Metformin inhibits gallbladder cancer.

Abstract

Gallbladder cancer (GBC) is the most common biliary tract cancer with poor prognosis and wide variation in incidence rates worldwide, being very high in some countries in Latin America and Asia. Treatment of type 2 diabetes with metformin causes a reduction in the incidence of cancer. Till date, there are no reports on the anti-tumor effects of metformin in gall bladder cancer. Therefore, this study evaluated the effects of metformin on the proliferation of human gallbladder adenocarcinoma cells *in vitro* and *in vivo*, as well as explored the microRNAs associated with the anti-tumor effects of metformin. Metformin inhibited the proliferation in gallbladder adenocarcinoma cell lines NOZ, TGBC14TKB, and TGBC24TKB, and blocked the G0 to G1 transition in the cell cycle. This was accompanied by strong reduction in the expression of G1 cyclins, especially cyclin D1 and its catalytic subunits including cyclin-dependent kinase (Cdk) 4, and in retinoblastoma protein phosphorylation (p-Rb). In addition, metformin reduced the phosphorylation of receptor tyrosine kinases (RTK), especially Tie-2, ALK, PYK, EphA4, and EphA10, as well as angiogenesis-related proteins, including RANTES, TGF-β, and TIMP-1. Moreover, metformin also markedly altered

microRNA expression profile leading to an anti-tumor effect. Treatment of athymic nude mice bearing xenograft tumors with metformin inhibited tumor growth. These results suggest that metformin may be used clinically for the treatment of gallbladder adenocarcinoma.

Keywords: gallbladder cancer; metformin; cell cycle; microRNAs

Introduction

Gallbladder cancer (GBC) is the fifth most common neoplasm of digestive and biliary tract, and is the most common biliary tract malignancy [1-3]. The global incidence rates of GBC vary widely, being low in several European countries and the United States, relatively high in some central and eastern European countries, and very high in some countries in Latin America and Asia [4]. The prognosis for GBC is poor and the overall 5-year survival rate is less than 5 % [5]. In addition, the rate of GBC occurring in conjugation with diabetes is high [6, 7]. Thus, if an anti-diabetic drug is effective for both gallbladder cancer and diabetes, use of such a drug provides double benefits to the patient.

Metformin is an oral anti-hyperglycemic agent of the biguanide family, and the most commonly prescribed medication for the treatment of type-2 diabetes mellitus (DM) [8]. According to epidemiological studies, DM is a risk factor for biliary tract malignancies, including intrahepatic and extrahepatic cholangiocarcinoma (CCA), and GBC [6, 7]. In previous investigations, metformin has been shown to inhibit cell proliferation in various cancer types, including prostate cancer [9], breast cancer [10], pancreas cancer

[11], gastric cancer [12], esophageal cancer [13], and hepatocellular carcinoma [14, 15]. Recently, metformin has been shown to exhibit therapeutic potential against biliary tract malignancies [16].

Metformin exhibits antitumor effects including activation of 5'-AMP-activated protein kinase (AMPK) [17]. Metformin-induced activation of AMPK has been correlated with cell cycle arrest, apoptosis, and inhibition of protein synthesis [18]. We reported that metformin causes G0/G1 cell cycle arrest via downregulation of cyclin D1 [12-16]. CyclinD1 is a key regulator of G0/G1 arrest, and its overexpression is correlated with poor prognosis and chemoresistance in biliary tract malignancies [19-21]. Therefore, arrest of cell cycle progression might be an effective strategy for treatment of GBC. Recent studies have shown that metformin inhibits cell proliferation and tumor growth in human CCA through G0/G1 arrest by decreasing the protein levels of cyclins and cyclin dependent kinases (Cdk). However, the anti-tumor effect of metformin and its mechanism of action in CCA are currently unclear.

This study aimed to evaluate the mechanism of metformin`s antitumor effect on gallbladder adenocarcinoma cell line and its effect on miRNA expression profile.

Materials and Methods

Regents and antibodies

Metformin (1,1-dimethylbiguanide monohydrochloride) was purchased from Astellas Pharma Inc. (Tokyo, Japan). Cell counting kit (CCK-8) was purchased from Dojindo Laboratories (Kumamoto, Japan), and all other chemicals were obtained from Sigma Chemical (Tokyo, Japan).

The primary antibodies used for western blot analyses were obtained from the following sources: antibodies against cyclin D1 and cyclin E were obtained from Thermo Fisher Scientific (Walthman, MA, USA); antibodies against Cdk4 were obtained from Cell Signaling Technology (Denvers, MA, USA); antibodies against Cdk2, Cdk6, and retinoblastoma proteins (Rb) were obtained from Santa Cruz Biotechnology (Santa Cruz, CA, USA); antibodies against phosphorylated retinoblastoma proteins (phospho-Rb) were obtained from BD Pharmingen (San Diego, CA, USA).

Secondary antibodies included horseradish peroxidase (HRP)-linked anti-mouse and

anti-rabbit IgG antibodies (Cell Signaling Technology, USA).

Cell culture and cell proliferation assay

The human GBC cell line NOZ was obtained from the Japanese Collection of Research Bioresources (Osaka, Japan). The GBC cell lines TGBC14TKB and TGBC24TKB were obtained from Riken Cell Bank (Tsukuba, Japan). NOZ was cultured in Williams' medium E (Gibco Invitrogen, Carlsbad, CA) supplemented with 10 % fetal bovine serum (FBS) and penicillin-streptomycin 100 mg/L (Invitrogen). TGBC14TKB and TGBC24TKB were cultured in Dulbecco's modified Eagle's medium (Gibco, Tokyo, Japan) supplemented with 10 % fetal bovine serum (FBS) and penicillin-streptomycin 100 mg/L (Invitrogen) at 37 °C in a humidified atmosphere containing 5 % CO_2.

Cell proliferation assay was performed using the CCK-8 cell counting kit, according to the manufacturer's instructions. Briefly, 5×10^3 cells were seeded into each well of a 96-well plate and cultured in 100 μL of 10 % FBS containing the each medium for 24 h. Subsequently, the seeded cells were cultured with metformin (1, 5, and 10 mmol/L) or

without metformin for 72 h. CCK-8 reagent (10 μL) was added to each well, and the plates were then incubated at 37 °C for 3 h. The absorbance of each well was measured at 450 nm using a microplate reader.

Flow cytometric analysis

In order to elucidate the mechanism of antitumor effects of metformin, its influence on the cell cycle was examined using flow cytometric analysis. NOZ cells (1.0×10^6 cells in a 100 mm diameter dish) were cultured with 10 mmol/L metformin or without metformin for 24 h. Treated cells were washed with PBS and then stored at −20 °C. On the day of analysis, the cells were washed with cold PBS, suspended in a mixture of 100 μL PBS and 10 μL RNaseA (250 μg/mL), and incubated for 30 min at 37°C. Then, 110 μL propidium iodide (PI) staining solution (100 μg/ml) was added to each tube, and the cells were incubated at 4 °C for more than 30 min before analysis. Flow cytometry was performed using a Cytomics FC 500 flow cytometer (Beckman Coulter, Indianapolis, IN, USA) with an argon laser (488 nm). The percentages of cells in different phases of the cell cycle were evaluated by FlowJo software (TreeStar, Ashland, OR, USA). All

experiments were performed in triplicates to ensure consistency of the results.

Gel electrophoresis and Western blotting

NOZ cells (1.0×10^6/dish) were seeded in 100 mm culture dishes and cultured for 24 h. The cells were further cultured either with 10 mmol/L metformin or without metformin for 24-72 h. The treated cells were lysed using PROPREP protein extraction solution (complete protease inhibitor mixture; iNtRON Biotechnology, Sungnam, Korea) on ice for 20 min. The cell lysates were then centrifuged at 13000 ×*g* at 4 °C for 5 min, and the supernatants containing soluble cellular proteins were collected and stored at −80 °C until further use. Protein concentrations were measured using a Nanodrop 2000 spectrofluorometer (Thermo Scientific Corporation, USA). Aliquots of protein were prepared in sample buffer and separated on 10 % Tris-glycine gradient gels by SDS-PAGE [22], followed by transfer to nitrocellulose membranes. After blocking, the membranes were incubated with primary antibodies, and then with HRP-conjugated secondary antibodies [23]. Immune reaction proteins were visualized on X-ray film with enhanced chemiluminescence detection system (Perkin Elmer Co., Waltham, MA).

Antibody arrays of phosphorylated receptor tyrosine kinase (p-RTK)

NOZ cells were cultured either with 10 mmol/L metformin or without metformin for 48 h. The cells were collected and lysed in PROPREP protein extraction solution. Human p-RTK was assayed using the Human p-RTK Array Kit (R&D systems, Minneapolis, MN, USA) according to the manufacturer's instructions. The densities of the immunoreactive bands obtained in this array were analyzed by densitometric scanning (TIc scanner, Shimizu Co, Ltd., Kyoto, Japan).

Angiogenic profile analysis using an antibody array

The RayBio Human Angiogenesis Antibody Array (RayBiotech Inc., GA, USA) was used according to the manufacturer's protocol. This method is a dot-based assay enabling the detection and comparison of 20 angiogenesis-specific cytokines. The densities of the immunoreactive spots obtained on this array were evaluated by densitometric scanning (TIc scanner, Shimizu Co, Ltd., Kyoto, Japan).

Analysis of miRNA arrays

The cancer cell lines were processed for total RNA extraction with the miRNeasy Mini Kit (Qiagen) according to the manufacturer`s instructions. The used samples typically showed $A_{260/280}$ ratios between 1.9 and 2.1, using an Agilent 2100 Bioanalyzer (Agilent Technologies, Santa Clara, CA, USA).

After evaluation of RNA concentration with an RNA 6000 Nano kit (Agilent Technologies), the samples were labeled using an miRCURYHy3/Hy5 Power Labeling Kit and were hybridized to a human miRNA Oligo chip (v.21.0; Toray Industries, Tokyo, Japan). The chips were then scanned with a 3-D Gene Scanner 3000 (Toray Industries), and the results were analyzed using 3D-Gene extraction software version 1.2 (Toray Industries). Differences in miRNA expression between samples treated and not-treated with metformin were measured by analyzing the raw data using GeneSpringGX v10.0 (Agilent Technologies). First, the samples were normalized to 28S rRNA values, and then, the baseline was corrected to the median of all samples.

Replicate data was consolidated into 2 groups: from metformin-treated cells and cells not-treated with metformin, and organized using the hierarchical clustering and

ANOVA functions in GeneSpring software. Hierarchical clustering was performed using the “use clustering” function (condition tree) and Euclidean correlation as a distance metric. Two-way ANOVA and asymptotic *P* value computation without any error correction on the samples was performed to determine the miRNAs that varied most prominently across the groups. The *p* value cutoff was set to 0.05. Only > 50 % changes for at least one of the time points for each sample were considered significant. All the analyzed data were scaled by global normalization. The statistical significance of differentially expressed miRNAs was analyzed by Student’s *t*-test.

Xenograft model analysis

Animal experiments were performed according to the guidelines of the Committee on Experimental Animals at Kagawa University, Kagawa, Japan. We purchased 27 male athymic mice (BALB/c-nu/nu; 7 weeks old; 20–25 g) from Japan SLC Inc. Athymic mice were kept under pathogen-free conditions in a laminar airflow rack and were placed in an environment where they could consume sterile food (γ-ray-irradiated food, CL-2; CLEA Japan Inc.) or autoclaved water at any time. Each mice were

subcutaneously inoculated with NOZ cells (5×10^6 cells per animal) in the flank. After one week, the xenografts became visible with a maximum diameter of 5 mm or more. The animals were randomly assigned to three groups with six animals per group. These groups were injected intraperitoneally (i.p.) with 1 mg metformin, 2 mg metformin, or control (PBS only), respectively, five times a week. Tumor growth was monitored daily by the same investigators (T. Yamashita and T. Masaki), and tumor size was measured weekly using the two greatest perpendicular dimensions. Tumor volume (mm^3) was calculated as [tumor length (mm) × tumor width $(mm)^2$]/2 [24]. All animals survived until day 24 of treatment, at which point they were sacrificed. Inter-group differences in tumor growth were analyzed by one-way ANOVA.

Statistical analysis

Each experiment was performed at least three times. Data was reported as mean ± SD. The statistical significance of the differences was analyzed using Student's *t*-test. *P* value < 0.05 was considered as statistically significant. All statistical analyses were performed using JMP 9.0 software (SAS Institute, Cary, NC).

Results

Metformin inhibits the proliferation of human gallbladder cancer cells

To evaluate the antitumor effect of metformin on the growth of human gallbladder cancer cells *in vitro*, we first examined the effects of metformin on the proliferation of three gallbladder cancer cell lines, NOZ, TGBC14TKB, and TGBC24TKB. Cells were grown in 10 % FBS and treated with either metformin (1, 5, or 10 mmol/L) or control (without metformin) for 72 h. As shown in Fig. 1, metformin (1, 5, and 10 mmol/L) caused a dose- and time-dependent decrease in the proliferation of all three cell lines. In summary, the results demonstrated that metformin inhibited gall bladder cancer cell proliferation.

Effects of metformin on cell-cycle regulatory proteins in NOZ cells

In order to investigate the cause of suppression of growth of NOZ cells due to metformin, cell-cycle related proteins were examined by flow cytometry. Fig. 2A depicts the typical flow cytometric histogram.

We treated proliferating NOZ cells with 10 mmol/L metformin for different durations.

Seventy two hours after the addition of 10 mmol/L metformin, a higher number of cells (50.6 %) were arrested in the G0-G1 phase in the metformin treated group compared with 36.3 % cells in the control group (Fig. 2A). This was accompanied by reduction in the percentages of cells in the S- and G2-M phases. These data suggested that metformin induces G0/G1 arrest in cancer cells.

Furthermore, we investigated the effects of metformin on cell-cycle related proteins using western blotting. Cells were treated without or with 10 mmol/L metformin for 24–72 h. The most prominent metformin-related change was the loss of cyclin D1, an important protein involved in the transition from G0-G1 phase, which showed a time-dependent decrease in metformin treatment (Fig. 2B). Cdk4 expression was reduced at 72 h after treatment with metformin. However, cyclin E and Cdk6 levels were unchanged.

The substrate of cyclin D1/Cdk4 and cyclin D1/Cdk6 is Rb. Phosphorylated Rb was found to be progressively decreased in metformin-treated cells, but no effect on total Rb was observed, suggesting that the kinase activity of cyclin D1/Cdk4 and cyclin D1/Cdk6 was decreased.

Effects of metformin on p-RTKs *in vitro*

The antitumor effects of metformin on RTK were investigated using RTK array system. Using an antibody array (Fig. 3A) facilitated the screening of 49 activated RTKs in NOZ cells in the presence and absence of metformin. Metformin reduced the levels of phosphorylated Tie-2, PYK, ALK, EGFR, EphA4, and EphA10 *in vitro* (Fig. 3B). The densitometric ratios of Tie-2, PYK, ALK, EGFR, EphA4, and EphA10 spots in metformin-treated cells to those in untreated cells were 31.8 %, 32.1 %, 8.4 %, 72.1 %, 1.3 %, and 14.6 %, respectively (Fig. 3C).

Effects of metformin on angiogenesis *in vitro*

To investigate the effects of metformin on angiogenesis related molecules on NOZ cells, we used angiogenesis array system (Fig. 4A). Of the 20 angiogenesis molecules screened, the expressions of RANTES, TGF-beta, and TIMP were reduced by metformin treatment *in vitro* (Fig. 4B). The densitometric ratios of RANTES, TGF-beta, and TIMP spots in metformin-treated cells to untreated cells were 0.21 times, 20 times and 0.37 times, respectively (Fig. 4C).

Effects of metformin on miRNA expression profile

Using a custom microarray platform, we analyzed the expression levels of 2555 miRNAs in cell lines and tumor tissues in the presence and absence of metformin. Treatment of NOZ cells with 10 mmol/L metformin for 48 h significantly upregulated 12 miRNAs and significantly downregulated 23 miRNAs (Table 1).

Unsupervised hierarchical clustering analysis showed that cells treated *in vitro* with metformin were clustered together and separately from untreated cells (Fig. 5).

Metformin inhibits *in vivo* tumor growth

To determine whether metformin could affect tumor growth *in vivo*, nude mice were subcutaneously injected with NOZ cells, followed by i.p. injection of metformin. Based on the integrated tumor growth curves, treatment with 1 mg and 2 mg doses of metformin substantially inhibited tumor growth by 75 % and 64 % (Fig. 6A and B), respectively, compared with untreated control mice. The tumor volumes in 1 mg-treated and 2 mg-treated groups were significantly smaller than those in the control group (*$P <$ 0.01).

Throughout this study, metformin showed no apparent side effects on these mice and did not affect their weight. All animals survived throughout the experiment.

Discussion

Metformin is one of the most commonly used antidiabetic drugs. The mechanism of action of metformin has been reported to be stimulation of glucose uptake in muscle and liver, increase of oxidation of fatty acid etc. [25]. It has also been shown to inhibit cancer cell proliferation [9-14] in various cancers, including the prostate cancer [9], breast cancer [10], stomach cancer [12], esophagus cancer [13], and liver cancer [14].

GBC is more common in Latin America and Asia than in Europe and the United States, it has poor prognosis, and its incidence is high in diabetic patients. Therefore, it would be very useful if the antitumor effects of metformin on gallbladder cancer could be elucidated.

The present findings are significant because 1) we demonstrated, for the first time, that metformin has an anti-tumor effect on GBC cells *in vitro* and *in vivo*; 2) it induces G0/G1 cell cycle arrest associated with modulation of cell cycle-regulatory protein

expression *in vitro*; and 3) it markedly suppresses the growth of subcutaneous GBC cells in athymic nude mice *in vivo*.

The expression of various cell-cycle-related molecules including cyclin D1 has been reported to be upregulated in various cancers [27-30]. In various cancer cells, metformin has been shown to downregulate cyclin D1 [9-14]. Therefore, inhibiting the expression of cell cycle-associated molecules, including cyclin D1, may lead to regulation of tumor growth. Complexes of Cdk4 and Cdk6 with cyclin D1 are necessary for G1 phase progression of the cell cycle, and further complexes of Cdk2 with cyclin E are required for the transition from G_1 phase to S phase [31, 32]. In the present study, metformin inhibited GBC cell cycle progression in the G0/G1 phase which correlated with a marked decrease in cyclin D1 expression. In addition, it was shown by flow cytometry, that metformin inhibits the transition from G0 to G1 phase in GBC cells *in vitro*. Therefore, major cell-cycle regulators (cyclin D1, Cdk4, and phosphorylated Rb) may be the intracellular targets of metformin resulting in an anti-proliferative effect in human GBC cell lines.

Our *in vitro* study was conducted using a higher dose of metformin than that used for

clinical treatment (6–30 μmol/L). Similar high doses have also been used in past reports [9, 10, 11]. However, cells in culture are grown under hyperglycemic conditions (high concentrations of glucose along with 5 % to 10 % FBS), resulting in excessive growth stimulation. This may explain why the anti-tumor effects of metformin in cell culture systems require higher doses than those used in patients with diabetes.

Previous studies have shown that metformin activates the AMPK pathway and inhibits p70S6K and mTOR phosphorylation in various cancers cells [25]. However, Ben Sahra *et al*. showed that the anti-proliferative effect of metformin is mediated via the mTOR pathway independent of AMPK [9]. In the present study, we did not observe significant changes in AMPKα and mTOR expression following metformin treatment in NOZ cells (data not shown). This discrepancy may be due to differences in the properties of various types of cancer cells.

Metformin has been found to alter the phosphorylation levels of RTKs, including EGFR and IGF1-R, in various cell lines [33]. In this study, we found that metformin reduced Tie-2, PYK, ALK, EGFR, EphA4, and EphA10 levels in GBC cells using protein arrays. In GBC, PTEN and TSC1 are frequently inactivated, whereas EGFR

family genes (EGFR, ERBB2, and ERBB3) are activated. The EGFR pathway is important in controlling cell cycle events. For example, EGFR activation was found to induce the expression of cyclin D1, a protein important for cell-cycle progression [34]. However, EphA4 [35], EphA10 [36], Tie-2 [37], PYK [38], and ALK [39] are frequently overexpressed in various human malignancies [33]. Thus, metformin may partially inhibit cell cycle related proteins via these tyrosine kinase signaling pathways in GBC cells.

The microenvironment also plays a key role in GBC pathogenesis by promoting tumor angiogenesis, invasion, and metastasis [40]. Using angiogenesis-related protein arrays, we demonstrated that metformin also reduced the levels of angiogenesis-related proteins such as RANTES [41], TGF-β [42], and TIMP-1 [43] in NOZ cells. RANTES, TGF-β, and TIMP-1 are associated with several malignancies, suggesting that reducing their expression is beneficial in patients with positive responses to chemotherapy, resulting in a lower risk of postoperative early recurrence [44, 45]. These results suggested that the antitumor effect of metformin may be due, at least in part, to the downregulation of angiogenesis-related molecules.

miRNAs associated with the anti-tumor effects of metformin were assessed using miRNA expression arrays. Cluster analyses clearly showed that metformin treatment affected the miRNA expression profile. We identified 35 miRNAs that were differentially expressed in the cluster. These miRNAs were potential candidates for assessing the efficacy of metformin treatment and may serve clues to the molecular basis of the anti-cancer effects of metformin, particularly those mediated by miRNAs.

miR-675-5p was reported as a functional target of the orphan G protein-coupled receptor 55 (GPR55), and has been shown to downregulate cyclinD1 and other molecules in non-small cell lung cancer [34]. It has also been reported that miR-675-5p is downregulated in adrenocortical cancer patients and metastatic prostate cancer cells [43-45]. The expression of miR-675-5p in patients with non-small cell lung cancer was negatively correlated with TNM stage and lymph node metastasis [43]. In the present study, metformin was found to upregulate miR-675-5p in NOZ cells, suggesting that miR-675-5p might be associated with the anti-tumor effect of metformin in GBC cells.

In conclusion, our results revealed that metformin inhibited human GBC cell proliferation and tumor growth, perhaps by suppressing cell-cycle-related molecules via

changes in miRNA expression profile. In the near future, the combination of metformin and standard chemotherapy drugs in many cancer types may be used to be synergistic effects to combat therapeutic resistance.

Acknowledgments

This work was supported by JSPS KAKENHI Grant Number JP18.

References

1 Bal MM, Ramadwar M, Deodhar K, Shrikhande S. Pathology of Gallbladder Carcinoma: Current Understanding and New Perspectives. Pathol Oncol Res. 2015;21:509-525.

2 Ha TY, Yoon YI, Hwang S, Park YJ, Kang SH, Jung BH, et al. Effect of Reoperation on Long-Term Outcome of pT1b/T2 Gallbladder Carcinoma After Initial Laparoscopic Cholecystectomy. J Gastrointest Surg. 2015;19:298–305.

3 Doval DC, Azam S, Sinha R, Batra U, Mehta A. Expression of epidermal growth factor receptor, p53, Bcl2, vascular endothelial growth factor, cyclooxygenase-2, cyclin D1, human epidermal receptor-2 and Ki-67: Association with clinicopathological profiles and outcomes in gallbladder carcinoma. J Carcinog. 2014;13:10:3903-9.

4 Levy AD, Murakata LA, Rohrmann CA Jr. Gallbladder carcinoma: radiologic-pathologic correlation. Radiographics. 2001;21(2):295–314. questionnaire, 549–555.

5 Goetze TO. Gallbladder carcinoma: Prognostic factors and therapeutic options. World J Gastroenterol. 2015;21(43):12211–7.

6 Soraya J Kaewpitoon, Ryan A Loyd, Ratana Rujirakul, Sukij Panpimanmas, Likit Matrakool, Taweesak Tongtawee, et al. Benefits of Metformin Use for Cholangiocarcinoma. Asian Pac J Cancer Prev. 2015;16(18):8079–83.

7 Ren HB, Yu T, Liu C, Li YQ. Diabetes mellitus and increased risk of biliary tract cancer: systematic review and meta-analysis. Cancer Causes Control. 2011;22:837–47.

8 Palmer WC, Patel T. Are common factors involved in the pathogenesis of primary liver cancers? A meta-analysis of risk factors for intrahepatic cholangiocarcinoma. J Hepatol. 2012;57:69–76.

9 Ben Sahra I, Laurent K, Loubat A, Giorgetti-Peraldi S, Colosetti P, Auberger P, et al. The antidiabetic drug metformin exerts an antitumoral effect in vitro and in vivo through a decrease of cyclin D1 level. Oncogene. 2008;27:3576–86.

10 Anisimov VN, Egormin PA, Piskunova TS, Popovich IG, Tyndyk ML, Yurova MN, et al. Metformin extends life span of HER-2/neu transgenic mice and in combination with melatonin inhibits growth of transplantable tumors in vivo. Cell Cycle. 2010;9:188–97.

11 Z Bao B, Wang Z, Ali S, Ahmad A, Azmi AS, Sarkar SH, et al. Metformin Inhibits

Cell Proliferation, Migration and Invasion by Attenuating CSC Function Mediated by Deregulating miRNAs in Pancreatic Cancer Cells. Cancer Prev Res (Phila). 2012;5(3):355–64.

12 Kato K, Gong J, Iwama H, Kitanaka A, Tani J, Miyoshi H, et al. The antidiabetic drug metformin inhibits gastric cancer cell proliferation in vitro and in vivo. Mol Cancer Ther. 2012;11:549–60.

13 Fujihara S, Kato K, Morishita A, Iwama H, Nishioka T, Chiyo T, et al. Antidiabetic drug metformin inhibits esophageal adenocarcinoma cell proliferation in vitro and in vivo. Int J Oncol. 2015;46(5):2172–80.

14 Miyoshi H, Kato K, Iwama H, Maeda E, Sakamoto T, Fujita K, et al. Effect of the anti-diabetic drug metformin in hepatocellular carcinoma in vitro and in vivo. Int J Oncol. 2014;45:322–32.

15 Morishita A, Masaki T. miRNA in hepatocellular carcinoma. Hepatol Res. 2015;45:128–41.

16 Fujimori T, Kato K, Fujihara S, Iwama H, Yamashita T, Kobayashi K, et al. Antitumor effect of metformin on cholangiocarcinoma: In vitro and in vivo studies.

Oncol Rep. 2015;34(6):2987–96.

17 Pernicova I, Korbonits M. Metformin-mode of action and clinical implications for diabetes and cancer. Nat Rev Endocrinol. 2014;10:143–56.

18 Kourelis TV, Siegel RD. Metformin and cancer: new applications for an old drug. Med Oncol. 2012;29:1314–27.

19 Hui AM, Cui X, Makuuchi M, Li X, Shi YZ, Takayama T. Decreased p27(Kip1) expression and cyclin D1 overexpression, alone and in combination, influence recurrence and survival of patients with resectable extrahepatic bile duct carcinoma. Hepatology. 1999;30(5):1167–73.

20 Sugimachi K, Aishima S, Taguchi K, Tanaka S, Shimada M, Kajiyama K, et al. The role of overexpression and gene amplification of cyclin D1 in intrahepatic cholangiocarcinoma. J Hepatol. 2001;35(1):74–9.

21 Ling S, Feng T, Ke Q, Fan N, Li L, Li Z, et al Metformin inhibits proliferation and enhances chemosensitivity of intrahepatic cholangiocarcinoma cell lines. Oncol Rep. 2014;31(6):2611–8.

22 Laemmli UK. Cleavage of structural proteins during the assembly of the head of

bacteriophage T4. Nature. 1970;227:680–5.

23 Towbin H, Staehelin T, Gordon J. Electrophoretic transfer of proteins from polyacrylamide gels to nitrocellulose sheets: procedure and some applications. Proc Natl Acad Sci USA. 1979;76:4350–4.

24 D'Incalci M, Colombo T, Ubezio P, Nicoletti I, Giavazzi R, Erba E, et al. The combination of yondelis and cisplatin is synergistic against human tumor xenografts. Eur J Cancer. 2003;39:1920–6.

25 Zhou G, Myers R, Li Y, Chen Y, Shen X, Fenyk-Melody J, et al. Role of AMP-activated protein kinase in mechanism of metformin action. J Clin Invest. 2001;108(8):1167–74.

26 Chaiteerakij R, Yang JD, Harmsen WS, Slettedahl SW, Mettler TA, Fredericksen ZS, et al. Risk factors for intrahepatic cholangiocarcinoma: association between metformin use and reduced cancer risk. Hepatology. 2013;57(2):648–55.

27 Han S, Kim HY, Park K, Lee MS, Kim HJ, Kim YD. Expression of p27Kip1 and cyclin D1 proteins is inversely correlated and is associated with poor clinical outcome in human gastric cancer. J Surg Oncol. 1999;71:147–54.

28 Aoyagi K, Koufuji K, Yano S, Murakami N, Terasaki Y, Yamasaki Y, et al. Immunohisto- chemical study on the expression of cyclin D1 and E in gastric cancer. Kurume Med J. 2000;47:199–203.

29 Masaki T, Shiratori Y, Rengifo W, Igarashi K, Yamagata M, Kurokohchi K, et al. Cyclins and cyclin- dependent kinases: Comparative study of hepatocellular carcinoma versus cirrhosis. Hepatology. 2003;37:534–43.

30 Masaki T, Shiratori Y, Rengifo W, Igarashi K, Matsumoto K, Nishioka M, et al. Hepatocellular carcinoma cell cycle: study of Long-Evans cinnamon rats. Hepatology. 2000;32:711–20.

31 Sherr CJ. Mammalian G1 cyclins. Cell. 1993;73:1059–65.

32 Sherr CJ. G1 phase progression: cyclin g on cue. Cell. 1994;79:551–5.

33 Pollak M. Insulin and insulin-like growth factor signaling in neoplasia. Nat Rev Cancer. 2008;8:915–28.

34 Narayanan R, Kim HN, Narayanan NK, Nargi D, Narayanan B. Epidermal growth factor-stimulated human cervical cancer cell growth is associated with EGFR and cyclin D1 activation, independent of COX-2 expression levels. Int J Oncol. 2011;40:13–20.

35 Oki M, Yamamoto H, Taniguchi H, Adachi Y, Imai K, Shinomura Y. Overexpression of the receptor tyrosine kinase EphA4 in human gastric cancers. World J Gastroenterol. 2008;14:5650–6.

36 Li Y, Jin L, Ye F, Ma Q, Yang Z, Liu D, et al. Isoform expression of EPHA 10 protein mediate breast cancer progression by regulating the E-cadherin and β-catenin complex. Oncotarget. 2017;8:30344–56.

37 Zhang JH, Wang LH, Li XJ, Wang AP, Reng LQ, Xia FG, et al. Expression of Ang-2/Tie-2 and PI3K/AKT in Colorectal Cancer. ASIAN PACIFIC JOURNAL OF CANCER PREVENTION. 2014:15:8651-6.

38 Lipimski CA, Tran NL, Menashi E, Rohl C, Kloss J, Bay RC, et al. The tyrosine kinase pyk2 promotes migration and invasion of grioma cells. Neoplasia. 2005;7:435–45.

39 Yoshida R, Sasaki T, Minami Y, Hibino Y, Okumura S, Sado M, et al. Activation of Src signaling mediates acquired to ALK inhibition in lung cancer. Int J Oncol. 2017;51:1533–40.

40 Simone V, Brunetti O, Lupo L, Testini M, Maiorano E, Simone M, et al. Targeting

Angiogenesis in Biliary Tract Cancers: An Open Option. Int J Mol Sci. 2017;18(2):418.

41 Lv D, Zhang Y, Kim HJ, Zhang L, Ma X. CCL5 as a potential immunotherapeutic target in triple-negative breast cancer. Cell Mol Immunol. 2013;10:30310.

42 Principe DR, Doll JA, Bauer J, Jung B, Munshi HG, Bartholin L, et al. TGF-β: duality of function between tumor prevention and carcinogenesis. J Natl Cancer Inst. 2014;106, doi:10.1093/jnci/djt369.

43 Gong Y, Scott E, Lu R, Xu Y, Oh WK, Yu Q. TIMP-1 promote accumulation of cancer associated fibroblast and cancer progression. PLoS One. 2013;8: e77366. 2013.

44 He D, Wang J, Zhang C, Shan B, Deng X, Li B, et al. Down-regulation of miR-675-5p contributes to tumor progression and development by targeting pro-tumorigenic GPR55 in non-small cell lung cancer. Mol Cancer. 2015;14:73.

45 Zhu M, Chen Q, Liu X, Sun Q, Zhao X, Deng R, et al. lncRNA H19/miR-675 axis represses prostate cancer metastasis by targeting TGFBI. FEBS J. 2014;281:3766–75.

46 Schmitz KJ, Helwig J, Bertram S, Sheu SY, Suttorp AC, Seggewiss J, et al. Differential expression of microRNA-675, microRNA-139-3p and microRNA-335 in benign and malignant adrenocortical tumours. J Clin Pathol. 2011;64:529–35.

Figure legends

Figure 1. Metformin inhibits the proliferation of cultured GBC cells. NOZ, TGBC14TKB, and TGBC24TKB cells were seeded in 96-well plates. Metformin (1, 5, and 10 mmol/L) or vehicle was added to the culture medium; cells were subjected to the CCK assay at 24–72 h after metformin treatment. Cell viability was assayed daily from 0 to 72 h; viability of metformin-treated cells at each time point differed significantly from the control cells ($P^* < 0.05$).

Figure 2. (A) Flow cytometric analysis of proliferating NOZ cells at 24 h after addition of 10 mmol/L metformin (Met). Metformin blocked the cell cycle at G0/G1. Results are representative of three independent experiments. (B) Expressions of cyclin D1, Cdk4, Cdk6, cyclin E, phosphorylated Rb (pRb), and Rb in NOZ cells at 24, 48, and 72 h after the addition of 10 mmol/L metformin. Protein expression was assayed by western blotting.

Figure 3. (A) Template showing the location of tyrosine kinase antibodies spotted onto a human phospho-RTK array. (B) Representative expression of various phosphorylated tyrosine kinase receptors in NOZ cells treated with or without metformin. (C) The densitometric of ratios p-Tie, p-PYK, p-ALK, p-EGFR, p-EphA4, and p-EphA10 spots of metformin-treated to untreated cells were 31.8 %, 32.1 %, 8.4 %, 72.1 %,1.3 %, and 14.6%, respectively.

Figure 4. (A) Template showing the location of angiogenesis related proteins spotted onto a human angiogenesis array. (B) Representative expression of various

angiogenesis-related proteins in NOZ cells treated with or without metformin. (C) The densitometric ratios of RANTES, TGF-β, and TIMP spots of the metformin-treated cells to untreated cells were 0.21 times,, 20 times and 0.37 times, respectively (Fig. 4C).

, respectively.

Figure 5. Hierarchical clustering of NOZ cells with and without metformin treatment. NOZ cells were clustered according to the expression profiles of 35 miRNAs differentially expressed in NOZ cells with and without metformin treatment. The analyzed samples are shown in columns and the miRNAs are presented in rows. The miRNA clustering color scale shown at the top depicts relative expression levels of the miRNAs, with red and blue representing high and low expression levels, respectively.

Figure 6. *In vivo* anti-tumor effects of metformin on established gall bladder cancer xenografts in nude mice. NOZ cells were implanted subcutaneously into the flanks of nude mice. When tumors became palpable, 0 or 2 mg metformin was injected intraperitoneally for 23 days, 5 times per week. (A) Representative images of gross

NOZ tumors from nude mice treated with vehicle (i) or 2 mg metformin (ii). (B) Tumor growth curves in control and metformin groups. Tumor volume (mm^3) was calculated as (tumor length (mm) × tumor width (mm) ^{2})/2. Tumors were significantly smaller in metformin-treated than in vehicle-treated mice. Each point represents the mean ± standard deviation of six animals. *P = 0.01 by two-way ANOVA

Table 1. Statistical results and chromosomal locations of miRNAs in NOZ cells treated with or without metformin.

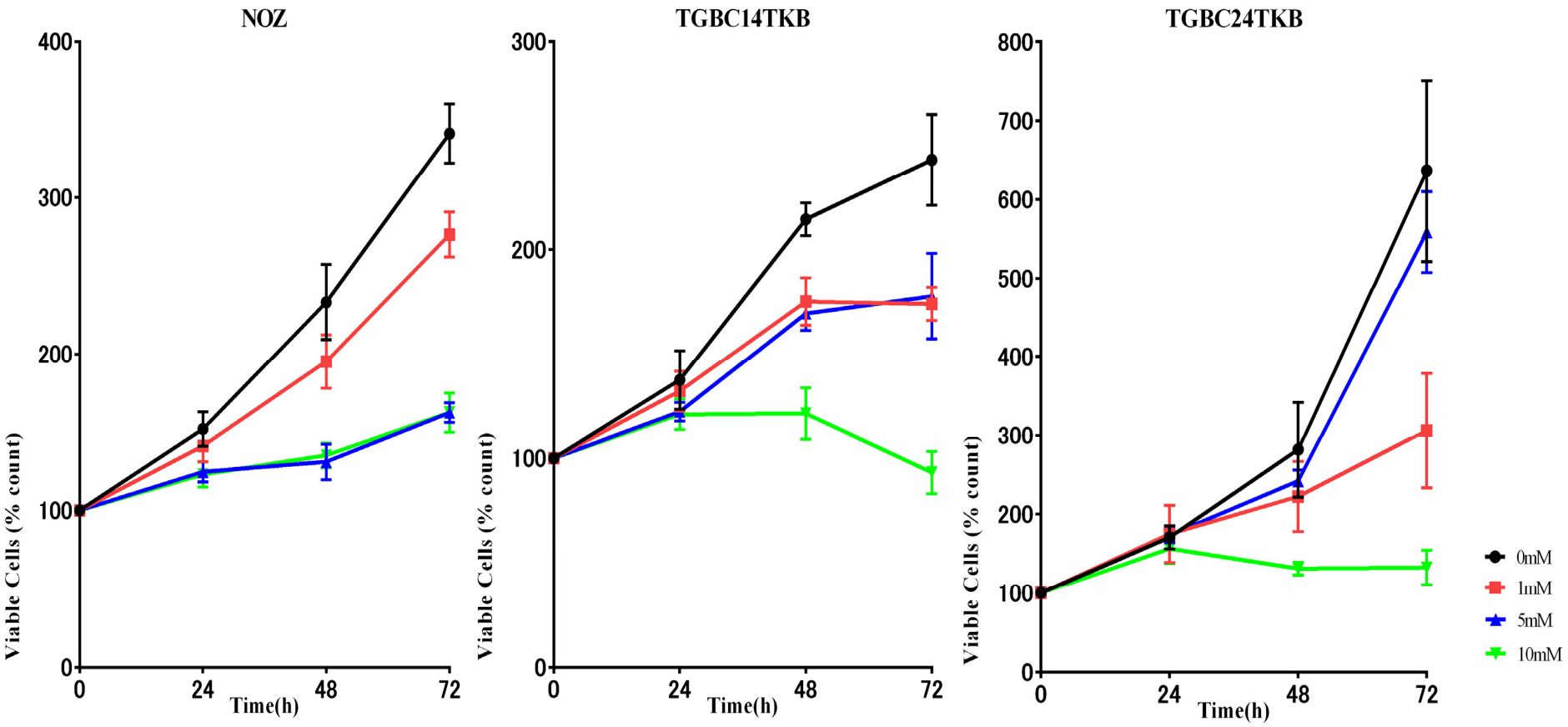
NOZ
TGBC14TKB
TGBC24TKB
Viable Cells (% count)
Time(h)
0
24
48
72
0mM
1mM
5mM
10mM

Figure 1

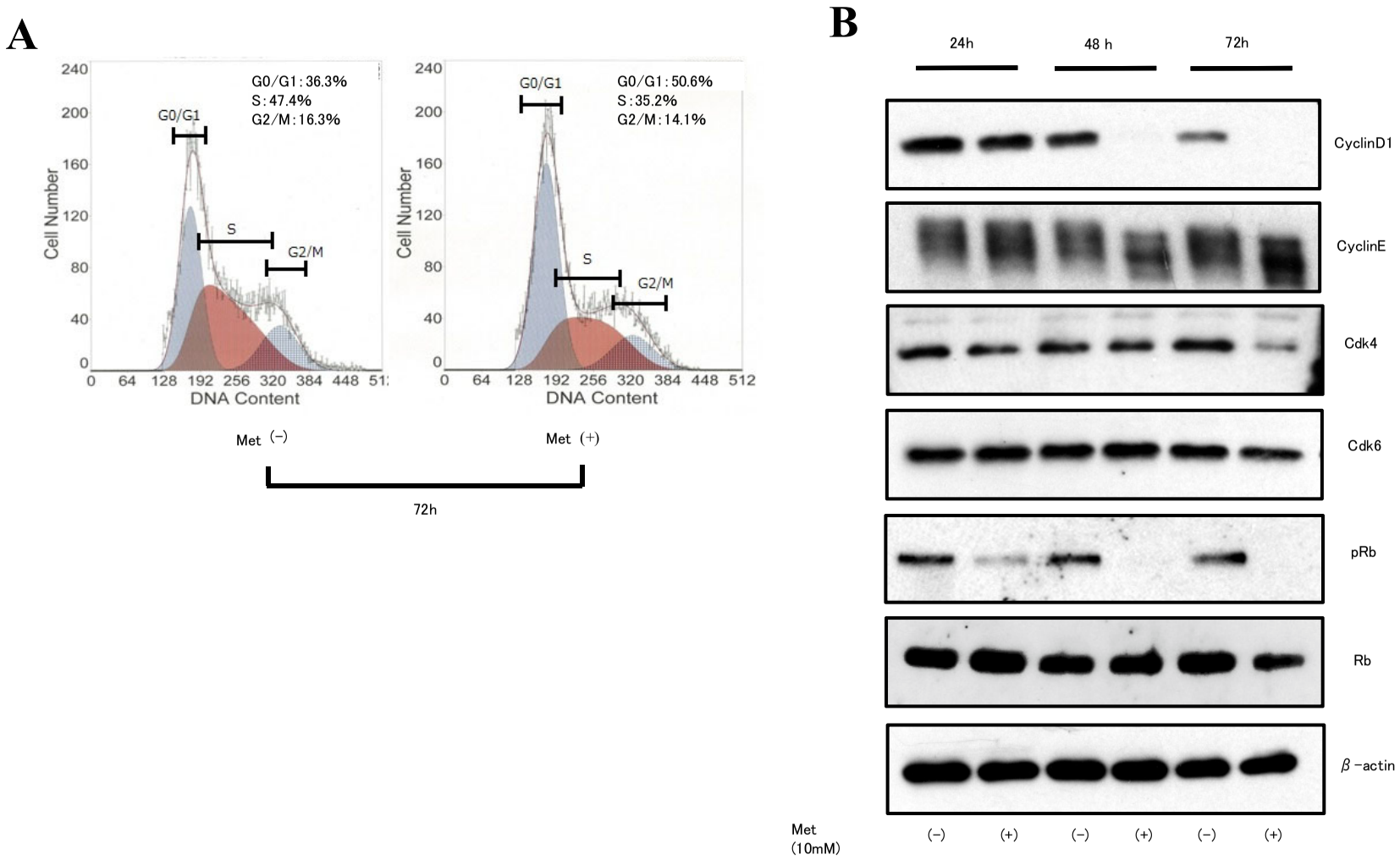
A
G0/G1 : 36.3%
S : 47.4%
G2/M : 16.3%
G0/G1
S
G2/M
Cell Number
DNA Content
G0/G1 : 50.6%
S : 35.2%
G2/M : 14.1%
Met (−)
Met (+)
72h
B
24h
48 h
72h
CyclinD1
CyclinE
Cdk4
Cdk6
pRb
Rb
β−actin
Met
(10mM)
(−) (+) (−) (+) (−) (+)

Figure 2

A

Reference Spots											Reference Spots
EGF R	ErbB2	ErbB3	ErbB4	FGF R1	FGF R2 α	FGF R3	FGF R4	Insulin R	IGF-1 R	Axl	Dtk
Mer	HGF R	MSP R	PDGF Rα	PDGF Rβ	SCF R	Flt-3	M-CSF R	C-Ret	ROR1	ROR2	Tie-1
Tie-2	TrkA	TrkB	TrkC	VEGF R1	VEGF R2	VEGF R3	MuSK	EphA1	EphA2	EphA3	EphA4
EphA6	EphA7	EphB1	EphB2	EphB4	EphB6	ALK	DDR1	DDR2	EphA5	EphA10	
Reference Spots		EphB3	PYK								PBS

B

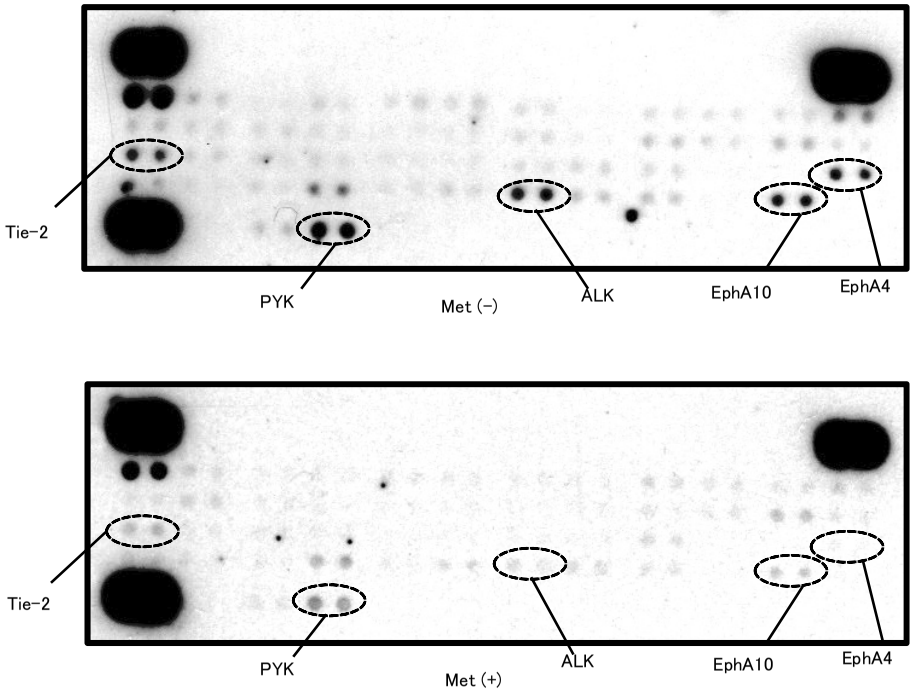

C

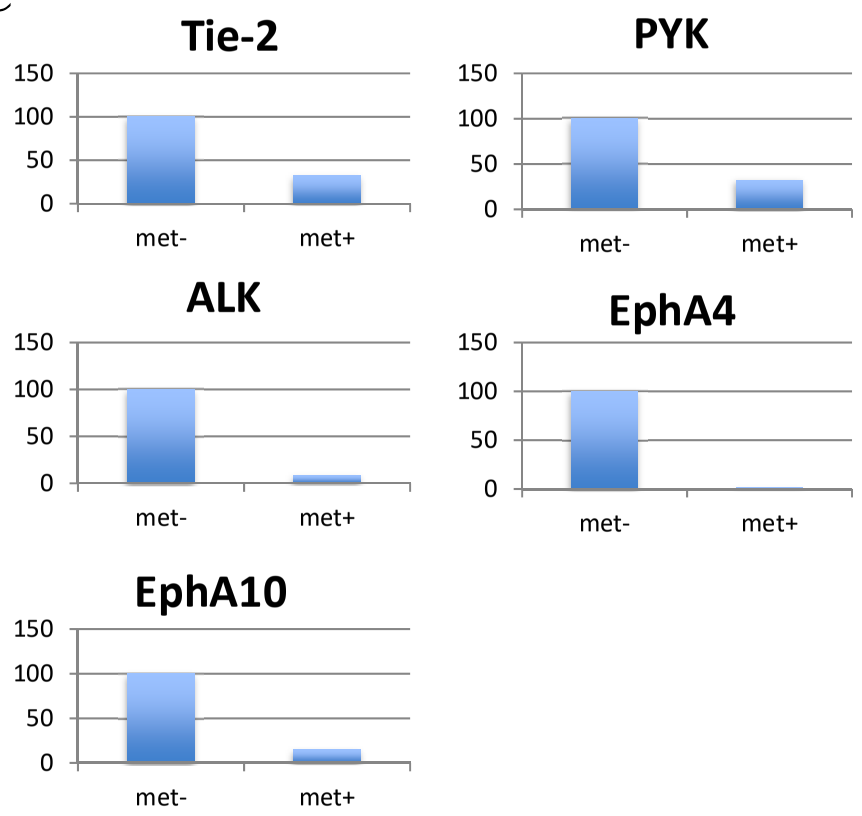

Figure 3

A

POS	POS	NEG	NEG	ANG	EGF	ENA-78	b FGF
POS	POS	NEG	NEG	ANG	EGF	ENA-78	b FGF
GRO	IFN gamma	IGF-1	IL-6	IL-8	Leptin	MCP-1	PDGF-BB
GRO	IFN gamma	IGF-1	IL-6	IL-8	Leptin	MCP-1	PDGF-BB
PLGF	RANTES	TGF beta 1	TIMP-1	TIMP-2	THPO	VEGF	VEGF-D
PLGF	RANTES	TGF beta 1	TIMP-1	TIMP-2	THPO	VEGF	VEGF-D
BLANK	BLANK	BLANK	BLANK	BLANK	BLANK	NEG	POS
BLANK	BLANK	BLANK	BLANK	BLANK	BLANK	NEG	POS

B

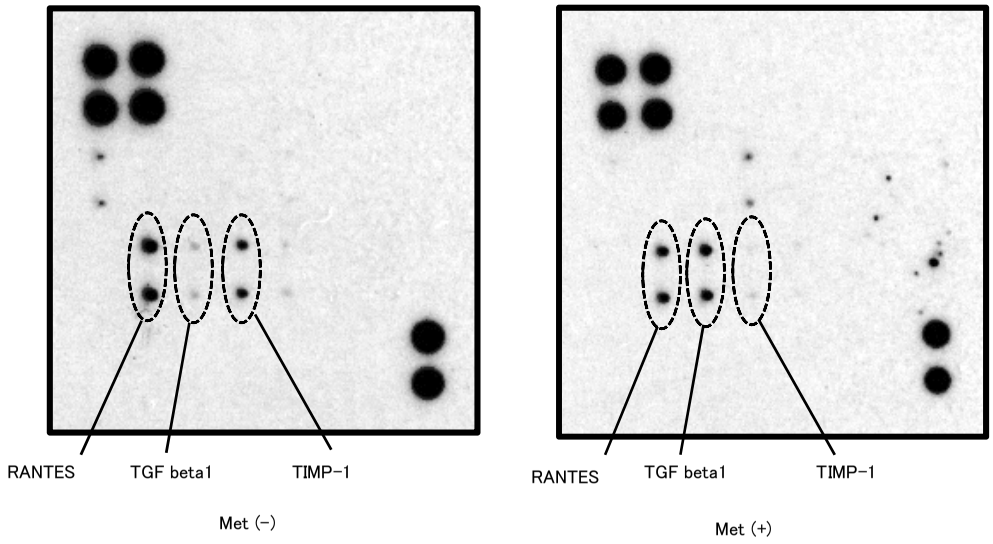

C

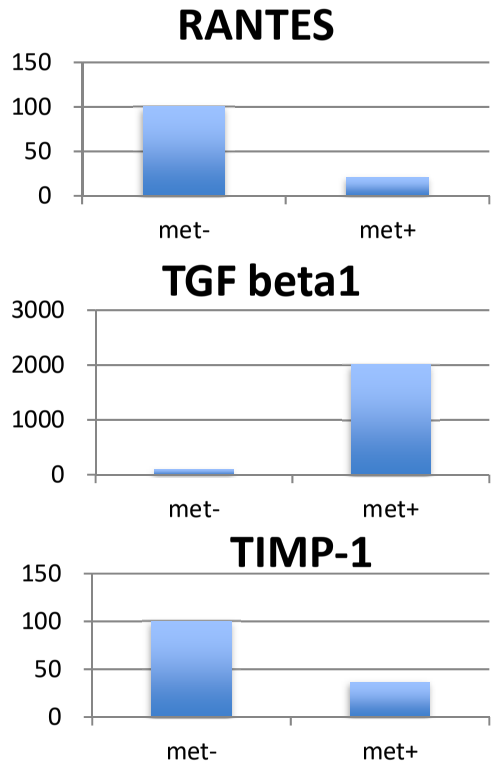

Figure 4

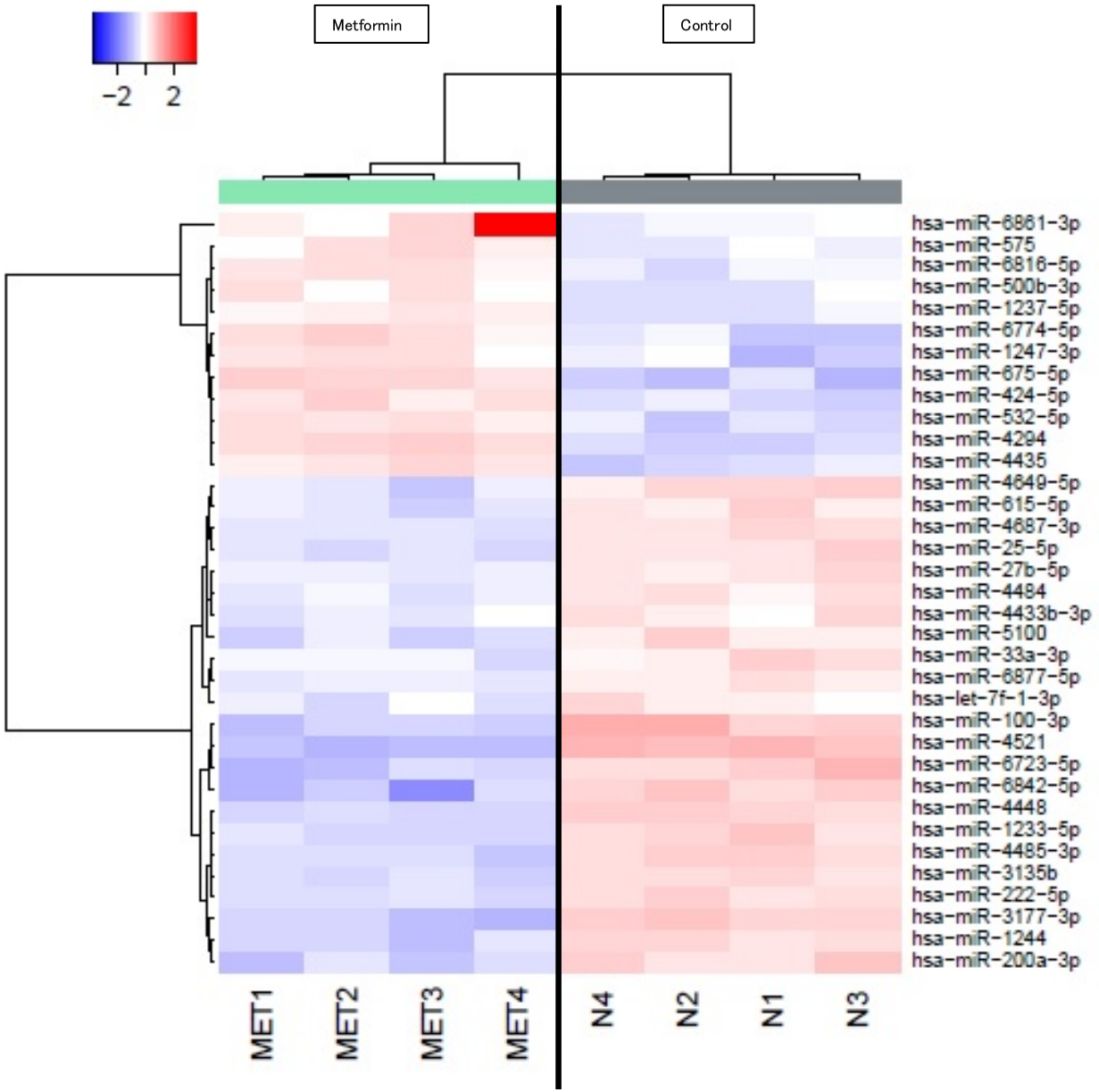
Metformin
Control
−2
2
hsa-miR-6861-3p
hsa-miR-575
hsa-miR-6816-5p
hsa-miR-500b-3p
hsa-miR-1237-5p
hsa-miR-6774-5p
hsa-miR-1247-3p
hsa-miR-675-5p
hsa-miR-424-5p
hsa-miR-532-5p
hsa-miR-4294
hsa-miR-4435
hsa-miR-4649-5p
hsa-miR-615-5p
hsa-miR-4687-3p
hsa-miR-25-5p
hsa-miR-27b-5p
hsa-miR-4484
hsa-miR-4433b-3p
hsa-miR-5100
hsa-miR-33a-3p
hsa-miR-6877-5p
hsa-let-7f-1-3p
hsa-miR-100-3p
hsa-miR-4521
hsa-miR-6723-5p
hsa-miR-6842-5p
hsa-miR-4448
hsa-miR-1233-5p
hsa-miR-4485-3p
hsa-miR-3135b
hsa-miR-222-5p
hsa-miR-3177-3p
hsa-miR-1244
hsa-miR-200a-3p
MET1
MET2
MET3
MET4
N4
N2
N1
N3

Figure 5

A

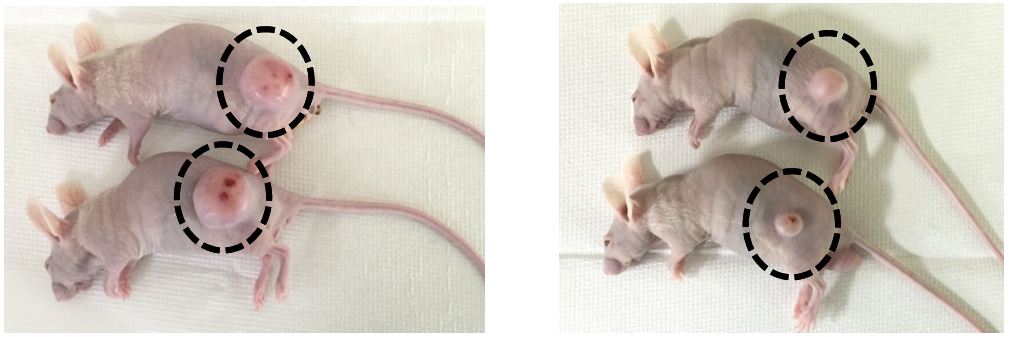

i) Control ii) Met 2 mg/d

B

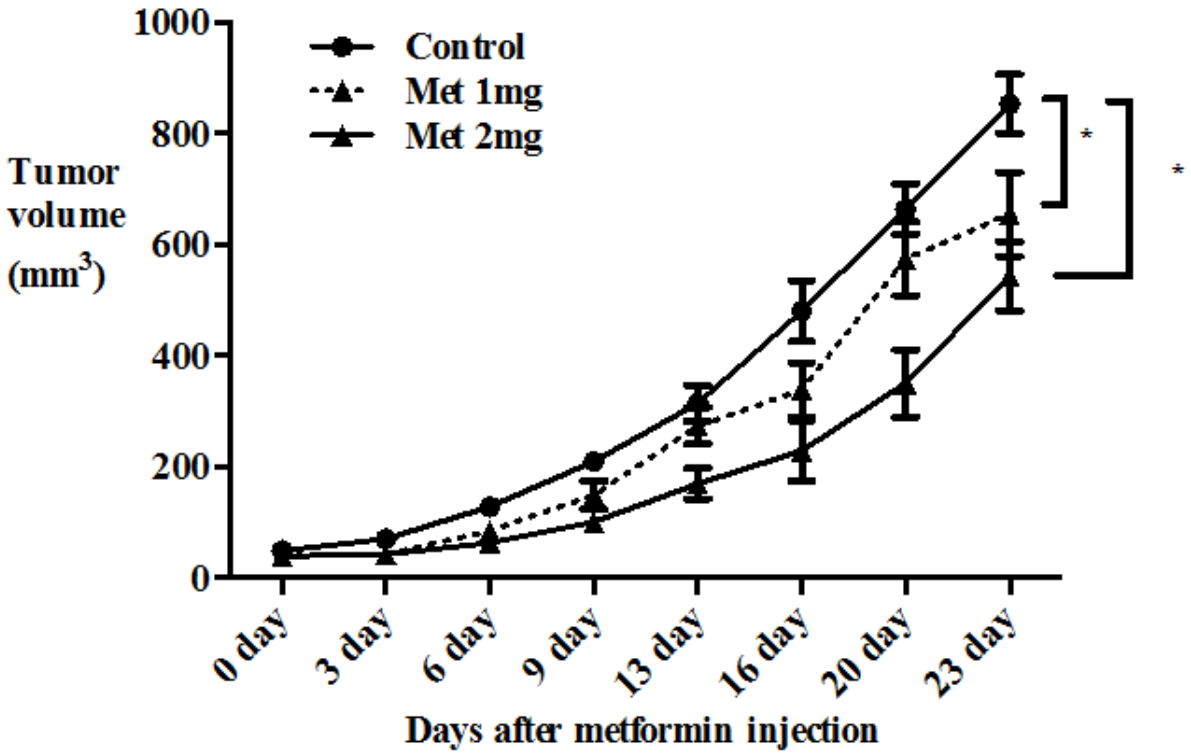

Figure 6